Journal of Naval Architecture and Marine Engineering
June, 2010
DOI: 10.3329/jname.v7i1.2901 http://www.banglajol.info

# RADIATION AND MASS TRANSFER EFFECTS ON MHD FREE CONVECTION FLOW PAST A MOVING VERTICAL CYLINDER IN A POROUS MEDIUM

**S. Suneetha and N. Bhaskar Reddy**

Department of Mathematics, Sri Venkateswara University, Tirupati - 517502, A.P., INDIA, Email: suneetha_svu@yahoo.co.in

## Abstract:

*The interaction of free convection with thermal radiation of a viscous incompressible unsteady MHD flow past a moving vertical cylinder with heat and mass transfer in a porous medium is analyzed. The fluid is a gray, absorbing-emitting but non-scattering medium and the Rosseland approximation is used to describe the radiative heat flux in the energy equation. The governing equations are solved by using an implicit finite-difference scheme of Crank-Nicolson type. The effects of various physical parameters such as thermal Grashof number, mass Grashof number, magnetic parameter, radiation parameter and Schmidt number on the velocity, temperature, concentration, local as well as average skin-friction, Nusselt number and Sherwood number for various parameters are computed and represented graphically. It is found that at small values of radiation parameter, the velocity and temperature of the fluid increases sharply near the cylinder as the time increases. Also, an increase in the magnetic field leads to a decrease in the velocity and a rise in the temperature. As the permeability parameter increases, it is seen that the flow accelerates. This model finds applications in geophysics and engineering.*

*Keywords:* Heat and Mass transfer, MHD, Porous medium, Radiation, Finite-difference Scheme, Vertical cylinder

## NOMENCLATURE

| | |
|---|---|
| $B_0$ | Magnetic induction |
| *cp* | specific heat at constant pressure |
| *C′* | dimensional species concentration |
| *C* | dimensionless species concentration |
| $D$ | Species diffusion coefficient |
| *g* | acceleration due to gravity |
| *Gr* | thermal Grashof number |
| *Gc* | solutal Grashof number |
| *k* | thermal conductivity |
| $k_e$ | mean absorption coefficient |
| K | the porous medium permeability coefficient |
| *M* | magnetic parameter |
| *N* | radiation parameter |
| $Nu_X$ | dimensionless local Nusselt number |
| $\overline{Nu}$ | dimensionless average Nusselt number |
| *Pr* | Prandtl number |
| R | dimensionless radial co-ordinate |
| $q_r$ | radiation heat flux |
| $r_0$ | radius of the cylinder |
| *Sc* | Schmidt number |
| $Sh_X$ | dimensionless local Sherwood number |
| $\overline{Sh}$ | dimensionless average Sherwood number |
| $t'$ | dimensional time |
| *t* | dimensionless time |
| $T'$ | temperature |
| $u_0$ | velocity of the cylinder |
| $u$ , $v$ | velocity components in $x$ , r directions respectively |
| *U,V* | dimensionless velocity components in X, R directions respectively |
| *x, y* | coordinates along and normal to the cylinder, respectively |
| *X, R* | dimensionless coordinates along and normal to the cylinder respectively |

***Greek symbols***

1813-8235 (Print), 2070-8998 (Online)  Received on: 25 July 2009

$\alpha$ thermal diffusivity
$\beta$ volumetric coefficient of thermal expansion
$\beta^*$ volumetric coefficient of expansion with concentration
$\mu$ dynamic viscosity
$\nu$ kinematic viscosity
$\rho$ density of the fluid,
$\sigma$ electrical conductivity
$\sigma_s$ Stefan-Boltzmann constant
$\tau'$ Local skin-friction
$\overline{\tau_L}$ average skin-friction
$\tau_X$ dimensionless local skin- friction
$\overline{\tau}$ dimensionless average skin-friction

***Subscripts***

*w* conditions on the wall
$\infty$ free stream conditions

## 1. Introduction

The study of unsteady boundary layer flow over a moving vertical cylinder has important geophysical and engineering applications. For example, as a result of volcanic activities or tectonic movements, magmatic intrusion may occur at shallow depths in the earth crust. The intrusive magma may take the form of a cylindrical shape. An experimental and analytical study is reported by Evan et al. (1968) for transient natural convection in a vertical cylinder. Velusamy and Grag (1992), given a numerical solution for the transient natural convection over a heat generating vertical cylinder.

The interaction of heat and mass transfer with magnetic field has attracted the interest of many researches in view of its applications in MHD generators, plasma studies, nuclear reactors, geophysics and astrophysics. Michiyoshi et al. (1976) considered natural convection heat transfer from a horizontal cylinder to mercury under a magnetic field. Shanker and Kishan (1997) presented the effect of mass transfer on the MHD flow past an impulsively started infinite vertical plate. Ganesan and Rani (2000) studied the effect of MHD on unsteady free convection flow past a vertical cylinder with heat and mass transfer. Magnetic field effect on a moving vertical cylinder with constant heat flux was given by Ganesan and Loganathan (2003).

In the context of space technology and in processes involving high temperatures, the effects of radiation are of vital importance in the study of geological formations, in the exploration and thermal recovery of oil, and in the assessment of aquifiers, geothermal reservoirs and underground nuclear waste storage sites. Here intrusive magma may be taken as an isothermal vertical cylinder with impulsive motion subject to radiative flux. The study of the flow along a vertical or horizontal cylinder is important in the field of geothermal power generation and drilling operations. Hossain et. al. (1999) studied Radiation-conduction interaction on mixed convection from a horizontal circular cylinder. Radiation and mass transfer effects on flow of an incompressible viscous fluid past a moving vertical cylinder was studied by Ganesan and Loganathan (2002). Mosa (1979) studied radiative heat transfer in horizontal magneto hydrodynamic channel flow with buoyancy effects and an axial temperature gradient. Radiation and mass transfer effects on two-dimensional flow past an impulsively started isothermal vertical plate were studied by Ramachandra Prasad et al. (2007).

In astrophysical regimes, the presence of planetary debris, cosmic dust etc. creates a suspended porous medium saturated with plasma fluids. Combined buoyancy-generated heat and mass transfer, due to temperature and concentration variations, in fluid-saturated porous media, has several important applications in a variety of engineering processes including heat exchanger devices, petroleum reservoirs, chemical catalytic reactors, solar energy porous water collector systems, ceremic materials(1992). Comprehensive reviews of the much of the work communicated in porous media thermal/species convection have been presented by Nield and Bejan (2006), Vafai (2005) and Ingham and Pop (2002). Yih (1999) studied the radiation effect on natural convection over a vertical cylinder embedded in porous media. More recently Nasser S. Elgazery and Hassan (2007) studied thermal radiation effect on magnetohydrodynamic (MHD) unsteady mixed-convection flow over a moving vertical cylinder with constant heat flux through a porous medium in the presence of transversal uniform magnetic field.

However, the interaction of radiation with mass transfer of an electrically conducting fluid past a vertical cylinder in a porous medium has received a little attention. Hence, the object of the present paper is to analyze

the radiation and mass transfer effects on MHD free convection flow of a viscous incompressible fluid past a verical cylinder in the presence of porous medium. The governing boundary layer equations along with the initial and boundary conditions are first cast into a dimensionless form and the resulting system of equations then solved by an implicit finite difference scheme.

## 2. Mathematical Analysis

A two-dimensional unsteady hydromagnetic flow of an incompressible viscous radiating fluid past an impulsively started semi-infinite vertical cylinder of radius $r_0$ in a porous medium is considered.

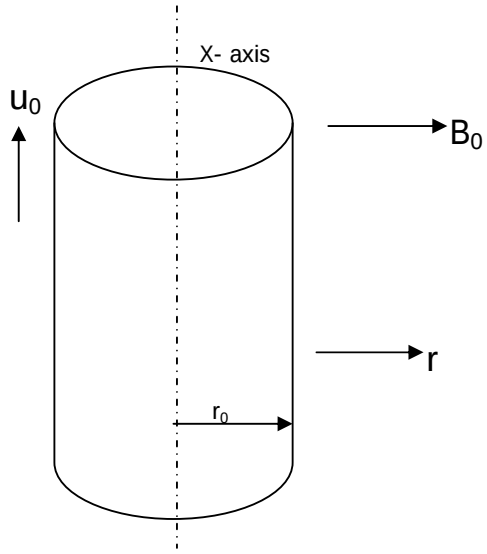


Figure.1 Physical model of the problem

Here the $x$-axis is taken along the axis of cylinder in the vertical direction and the radial coordinate $r$ is taken normal to the cylinder. This is shown in the figure.1. Initially, the fluid and the cylinder are of same temperature $T'_\infty$ and the concentration $C'_\infty$. At a time $t' \geq 0$, the cylinder starts moving in the vertical direction with velocity $u_0$. At a later time, the surface of cylinder is raised to a uniform temperature $T'_w$ and concentration $C'_w$ and are maintained constantly thereafter. A uniform magnetic field is applied in the transverse direction to the cylinder. The fluid is assumed to be slightly conducting, and hence the magnetic Reynolds number is much less than unity and the induced magnetic field is negligible in comparison with the transverse applied magnetic field. The viscous dissipation is also assumed to be neglected in the energy equation due to slow motion of the cylinder. It is assumed that the concentration $C'$ of the diffusing species in the binary mixture is very less in the comparison to the other chemical species, which are present, and hence the Soret and Dufour effects are negligible. All the physical properties are assumed to be constant except for the density in the buoyancy term. Then, under these assumptions and the Boussinesq's approximation, the flow is governed by the following system of equations:

Continuity equation

$$\frac{\partial (ru)}{\partial x} + \frac{\partial (rv)}{\partial r} = 0 \tag{1}$$

Momentum equation

$$\frac{\partial u}{\partial t'}+u\frac{\partial u}{\partial x}+v\frac{\partial u}{\partial r}=g\beta\left(T'-T'_\infty\right)+g\beta'\left(C'-C'_\infty\right)+\frac{\nu}{r}\frac{\partial}{\partial r}\left(r\frac{\partial u}{\partial r}\right)-\frac{\sigma B_0^2}{\rho}u-\frac{\nu}{K'}u \tag{2}$$

Energy equation

$$\frac{\partial T'}{\partial t'}+u\frac{\partial T'}{\partial x}+v\frac{\partial T'}{\partial r}=\frac{\alpha}{r}\frac{\partial}{\partial r}\left(r\frac{\partial T'}{\partial r}\right)-\frac{1}{\rho c_p}\frac{1}{r}\frac{\partial}{\partial r}\left(rq_r\right) \tag{3}$$

Mass diffusion equation

$$\frac{\partial C'}{\partial t'}+u\frac{\partial C'}{\partial x}+v\frac{\partial C'}{\partial r}=\frac{D}{r}\frac{\partial}{\partial r}\left(r\frac{\partial C'}{\partial r}\right) \tag{4}$$

The initial and boundary conditions are:

$$\begin{aligned}
&t'\le 0:\quad u=0,\ \ v=0,\ \ T'=T'_\infty,\quad C'=C'_\infty \quad \text{for all}\ \ x\ge 0 \ \text{and}\ r\ge 0\\
&t'>0:\quad u=u_0,\ \ v=0,\ \ T'=T'_w,\quad C'=C'_w \qquad\qquad at\quad r=r_0\\
&\qquad\quad u=0,\ \ T'=T'_\infty,\ C'=C'_\infty \qquad\qquad at\quad x\ =\ 0\\
&\qquad\quad u\to 0, T'\to T'_\infty,\ \ C'\to C'_\infty \qquad\qquad as\quad r\ \to\infty
\end{aligned} \tag{5}$$

We now assume Rosseland approximation (Brewster [13]), which leads to the radiative heat flux $q_r$ is given by

$$q_r=-\frac{4\sigma_s}{3k_e}\frac{\partial T'^4}{\partial y} \tag{6}$$

It should be noted that by using the Rosseland approximation, the present analysis is limited to optically thick fluids. If temperature differences within the flow are sufficiently small, then Equation (6) can be linearized by expanding $T'^4$ into the Taylor series about $T'_\infty$, which after neglecting higher order terms takes the form

$$T'^4\cong 4T'^3_\infty T'-3T'^4_\infty \tag{7}$$

In view of Equations (6) and (7), Equation (3) reduces to

$$\frac{\partial T'}{\partial t'}+u\frac{\partial T'}{\partial x}+v\frac{\partial T'}{\partial r}=\frac{\alpha}{r}\frac{\partial}{\partial r}\left(r\frac{\partial T'}{\partial r}\right)+\frac{16\sigma_s T'^3_\infty}{3k_e\rho c_p}\frac{1}{r}\frac{\partial}{\partial r}\left(r\frac{\partial T'}{\partial r}\right) \tag{8}$$

In order to write the governing equations and the boundary conditions in dimensionless form, the following non-dimensional quantities are introduced.

$$\begin{aligned}
&X=\frac{x\nu}{u_0 r_0^2},\quad R=\frac{r}{r_0},\quad t=\frac{t'\nu}{r_0^2},\quad U=\frac{u}{u_0},\quad V=\frac{\nu r_0}{\nu},Gr=\frac{g\beta r_0^2\left(T'_w-T'_\infty\right)}{\nu u_0},\\
&Gc=\frac{g\beta^* r_0^2\left(C'_w-C'_\infty\right)}{\nu u_0},\ N=\frac{4\sigma_s T'^3_\infty}{k_e k},\ M=\frac{\sigma B_0^2 r_0^2}{\rho\nu},\ T=\frac{T'-T'_\infty}{T'_w-T'_\infty}\\
&C=\frac{C'-C'_\infty}{C'_w-C'_\infty},\quad \Pr=\frac{\nu}{\alpha},\quad Sc=\frac{\nu}{D},\quad K=\frac{K'}{r_0^2}
\end{aligned} \tag{9}$$

Equations (1), (2), (8) and (4) are reduced to the following non-dimensional form

$$\frac{\partial(RU)}{\partial X}+\frac{\partial(RV)}{\partial R}=0 \tag{10}$$

$$\frac{\partial U}{\partial t}+U\frac{\partial U}{\partial X}+V\frac{\partial U}{\partial R}=GrT+Gc\ C+\frac{1}{R}\frac{\partial}{\partial R}\left(R\frac{\partial U}{\partial R}\right)-\left(M+\frac{1}{K}\right)U \tag{11}$$

$$\frac{\partial T}{\partial t}+U\frac{\partial T}{\partial X}+V\frac{\partial T}{\partial R}=\frac{1}{Pr}\left(1+\frac{4}{3}N\right)\frac{1}{R}\frac{\partial}{\partial R}\left(R\frac{\partial T}{\partial R}\right) \tag{12}$$

$$\frac{\partial C}{\partial t}+U\frac{\partial C}{\partial X}+V\frac{\partial C}{\partial R}=\frac{1}{Sc}\frac{1}{R}\frac{\partial}{\partial R}\left(R\frac{\partial C}{\partial R}\right) \tag{13}$$

The corresponding initial and boundary conditions are

$$\begin{aligned} &t\le 0:\ U=0,\ V=0,\ T=0,\ C=0 \\ &t>0:\ U=1,\ V=0,\ T=1,\ C=1 \qquad at \quad R=1 \\ &\qquad U=0,\ T=0,\ C=0 \qquad at \quad X=0 \\ &\qquad U\to 0,\ T\to 0,\ C\to 0 \qquad as \quad R\to\infty \end{aligned} \tag{14}$$

Knowing the velocity, temperature and concentration fields, it is interesting to study the local and average skin-friction, Nusselt number and Sherwood numbers are defined as follows.

Local and average skin-friction in non-dimensional form are given by

$$\tau_X=\frac{\tau'}{\rho u_0^2}=-\left(\frac{\partial U}{\partial R}\right)_{R=1} \tag{15}$$

$$\bar{\tau}=-\int_0^1\left(\frac{\partial U}{\partial R}\right)_{R=1}dX \tag{16}$$

Local and average Nusselt number in non-dimensional form are given by

$$Nu_X=-X\left(\frac{\partial T}{\partial R}\right)_{R=1} \tag{17}$$

$$\overline{Nu}=-\int_0^1\left(\frac{\partial T}{\partial R}\right)_{R=1}dX \tag{18}$$

Local and average Sherwood number in non-dimensional form are given by

$$Sh_X=-X\left(\frac{\partial C}{\partial R}\right)_{R=1} \tag{19}$$

$$\overline{Sh}=-\int_0^1\left(\frac{\partial C}{\partial R}\right)_{R=1}dX \tag{20}$$

## 3. Numerical Technique

In order to solve the unsteady, non-linear coupled Equations (10) to (13) under the conditions (14), an implicit finite difference scheme of Crank-Nicolson type has been employed. The region of integration is considered as a rectangle with sides $X_{\max}$ (=1) and $R_{\max}$ (=14), where $R_{\max}$ corresponds to $R=\infty$, which lies very well outside the momentum, energy and concentration boundary layers. The maximum of $R$ was chosen as 14 after some preliminary investigations, so that the last two of the boundary conditions (14) are satisfied within the tolerance limit $10^{-5}$.

The finite difference equations corresponding to Equations (10) to (13) are as follows:

$$\frac{\left[U_{i,j}^{n+1}-U_{i-1,j}^{n+1}+U_{i,j}^{n}-U_{i-1,j}^{n}+U_{i,j-1}^{n+1}-U_{i-1,j-1}^{n+1}+U_{i,j-1}^{n}-U_{i-1,j-1}^{n}\right]}{4\Delta X}+\frac{\left[V_{i,j}^{n+1}-V_{i,j-1}^{n+1}+V_{i,j}^{n}-V_{i,j-1}^{n}\right]}{2\Delta R}+\frac{V_{i,j}^{n+1}}{1+(j-1)\Delta R}=0 \tag{21}$$

$$\frac{\left[U_{i,j}^{n+1}-U_{i,j}^{n}\right]}{\Delta t}+U_{i,j}^{n}\frac{\left[U_{i,j}^{n+1}-U_{i-1,j}^{n+1}+U_{i,j}^{n}-U_{i-1,j}^{n}\right]}{2\Delta X}+V_{i,j}^{n}\frac{\left[U_{i,j+1}^{n+1}-U_{i,j-1}^{n+1}+U_{i,j+1}^{n}-U_{i,j-1}^{n}\right]}{4\Delta R}$$

$$= Gr\frac{\left[T_{i,j}^{n+1}+T_{i,j}^{n}\right]}{2}+Gc\frac{\left[C_{i,j}^{n+1}+C_{i,j}^{n}\right]}{2}+\frac{\left[U_{i,j-1}^{n+1}-2U_{i,j}^{n+1}+U_{i,j+1}^{n+1}+U_{i,j+1}^{n+1}-2U_{i,j}^{n}+U_{i,j+1}^{n}\right]}{2(\Delta R)^{2}}+$$

$$\frac{\left[U_{i,j+1}^{n+1}-U_{i,j-1}^{n+1}+U_{i,j+1}^{n}-U_{i,j-1}^{n}\right]}{4[1+(j-1)\Delta R]\Delta R}\ --\left(M+\frac{1}{K}\right)\left[U_{i,j}^{n+1}+U_{i,j}^{n}\right]\frac{1}{2} \tag{22}$$

$$\frac{[T_{i,j}^{n+1}-T_{i,j}^{n}]}{\Delta t}+U_{i,j}^{n}\frac{\left[T_{i,j}^{n+1}-T_{i-1,j}^{n+1}+T_{i,j}^{n}-T_{i-1,j}^{n}\right]}{2\Delta X}+V_{i,j}^{n}\frac{\left[T_{i,j+1}^{n+1}-T_{i,j-1}^{n+1}+T_{i,j+1}^{n}-T_{i,j-1}^{n}\right]}{4\Delta R}$$

$$=\frac{1}{\Pr}\left(1+\frac{4}{3}N\right)\frac{\left[T_{i,j-1}^{n+1}-2T_{i,j}^{n+1}+T_{i,j+1}^{n+1}+T_{i,j-1}^{n}-2T_{i,j}^{n}+T_{i,j+1}^{n}\right]}{2(\Delta R)^{2}}+\frac{\left[T_{i,j+1}^{n+1}-T_{i,j-1}^{n+1}+T_{i,j+1}^{n}-T_{i,j-1}^{n}\right]}{4\Pr[1+(j-1)\Delta R]\Delta R} \tag{23}$$

$$\frac{[C_{i,j}^{n+1}-C_{i,j}^{n}]}{\Delta t}+U_{i,j}^{n}\frac{\left[C_{i,j}^{n+1}-C_{i-1,j}^{n+1}+C_{i,j}^{n}-C_{i-1,j}^{n}\right]}{2\Delta X}+V_{i,j}^{n}\frac{\left[C_{i,j+1}^{n+1}-C_{i,j-1}^{n+1}+C_{i,j+1}^{n}-C_{i,j-1}^{n}\right]}{4\Delta R}$$

$$=\frac{1}{Sc}\frac{\left[C_{i,j-1}^{n+1}-2C_{i,j}^{n+1}+C_{i,j+1}^{n+1}+C_{i,j-1}^{n}-2C_{i,j}^{n}+C_{i,j+1}^{n}\right]}{2(\Delta R)^{2}}+\frac{\left[C_{i,j+1}^{n+1}-C_{i,j-1}^{n+1}+C_{i,j+1}^{n}-C_{i,j-1}^{n}\right]}{4Sc[1+(j-1)\Delta R]\Delta R} \tag{24}$$

Here, the subscript $i$ - designates the grid point along the $X$ - direction, $j$ - along the $R$ - direction and the superscript *n* along the *t* - direction. An appropriate mesh size considered for the calculation is $\Delta X$ = 0.05, $\Delta R$ = 0.25, and time step $\Delta t$ = 0.01. During any one-time step, the coefficients $U_{i,j}^{n}$ and $V_{i,j}^{n}$ appearing in the difference equations are treated as constants. The values of *U, V, T* and *C* are known at all grid points at *t* = 0 from the initial conditions. The computations of *U, V, T* and *C* at time level (*n+1*) using the known values at previous time level (*n*) are calculated as follows.

The finite difference Equation (24) at every internal nodal point on a particular $i$ - level constitute a tri-diagonal system of equations. Such a system of equations is solved by Thomas algorithm as described in Carnahan et al. [1969]. Thus, the values of *C* are found at every nodal point on a particular $i$ at $(n+1)^{th}$ time level. Similarly, the values of *T* are calculated from the Equation (23). Using the values of $C$ and *T* at $(n+1)^{th}$ time level in the Equation (22), the values of *U* at $(n+1)^{th}$ time level are found in a similar manner. Thus the values of *C, T* and *U* are known on a particular $i$ - level. The values of *V* are calculated explicitly using the Equation (21) at every nodal point on a particular $i$ - level at $(n+1)^{th}$ time level. This process is repeated for various $i$ - levels. Thus, the values of $C, T, U$ and $V$ are known at all grid points in the rectangular region at $(n+1)^{th}$ time level.

Computations are carried out till the steady state is reached. The steady state solution is assumed to have been reached, when the absolute difference between the values of *U* as well as temperature *T* and concentration *C* at two consecutive time steps are less than $10^{-5}$ at all grid points. The derivatives involved in the Equations (15) to (20) are evaluated using five-point approximation formula and the integrals are evaluated using Newton-Cotes closed integration formula. The truncation error in the finite-difference approximation is $O\left(\Delta t^{2}+\Delta R^{2}+\Delta X\right)$ and it tends to zero as $\Delta X$ , $\Delta R$ , $\Delta t \to 0$ . Hence the scheme is compatible. The finite-difference scheme is unconditionally stable as explained by Ganesan and Rani (2000). Stability and compatibility ensures convergence.

## 4. Results and Discussion

In order to get a physical insight into the problem, a representative set of numerical results in shown graphically in Figs. 2-10, to illustrate the influence of physical quantities such as radiation parameter *N*, thermal Grashof number *Gr*, mass Grashof number *Gc*, magnetic field parameter *M* , permeability coefficient *K* and Schmidt number *Sc* on velocity, temperature and concentration. All computations are carried out for Pr = 0.71(i.e., for air) and the corresponding values of Sc are chosen such that they represent water vapor (0.6) and carbon dioxide (0.94).

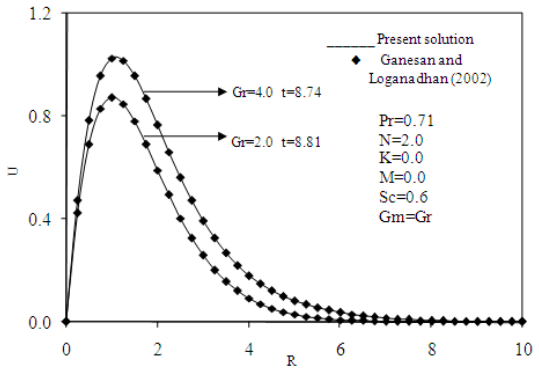


Fig. 2: Comparison of velocity profiles at X=1.0

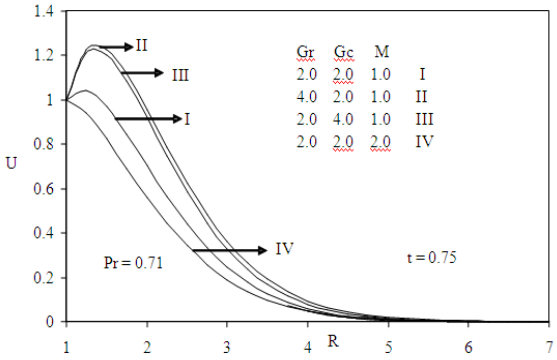


Fig.2(a): Transient velocity profiles at X=1.0 for different Gr, Gc and M

In order to ascertain the accuracy of the numerical results, the present study is compared with the previous study. The velocity profiles for Gr=2.0, 4.0, *Pr* = 0.71, *N* = 2.0, , K=0.0, *M* =0.0, Sc=0.6, Gr=Gm, *X* = 1.0 are compared with the available solution of Ganesan and Loganathan (2002) Fig.2. It is observed that the present results are in good agreement with that of Ganesan and Loganathan (2002).

The transient velocity profiles for different values of *Gr*, *Gc*, and *M* at a particular time $t = 0.75$ are shown in Fig.2(a). The thermal Grashof number signifies the relative effect of the thermal buoyancy (due to density differences) force to the viscous hydrodynamic force in the boundary layer flow. The positive values of *Gr* correspond to cooling of the cylinder surface by natural convection. Heat is therefore conducted away from the vertical cylinder into the fluid which increases temperature and thereby enhances the buoyancy force. It is observed that the transient velocity accelerates due to enhancement in the thermal buoyancy force, i.e., free convection effects. The solutal Grashof number *Gc* defines the ratio of the species buoyancy force to the viscous hydrodynamic force. It is noticed that the transient velocity increases considerbly with a rise in the species buoyancy force. In both the cases it is interesting to note that as *Gr* or *Gc* increases, there is rapid rise in the velocity near the surface of vertical cylinder and then descends smoothly to the free stream velocity. As expected, the transient velocity decreases with an increase in the magnetic parameter *M*. It is because that the application of transverse magnetic field will result a resistive type force (Lorentz force) similar to drag force which tends to resist the fluid flow and thus reducing its velocity. Also, the boundary layer thickness decreases with an increase in the magnetic parameter.

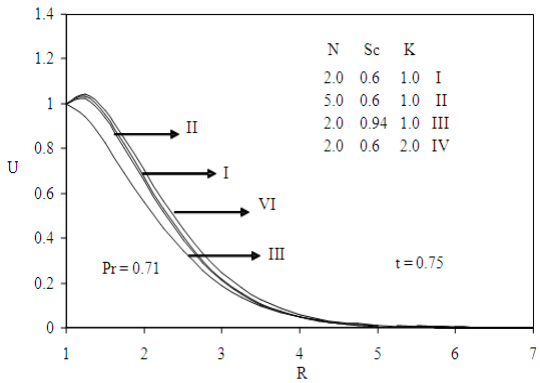


Fig.2(b): Transient velocity profiles at X=1.0 for different N, Sc and K

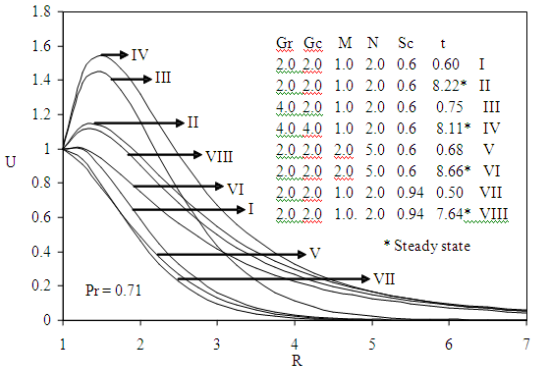


Fig.2(c): Velocity profiles at X=1.0 for different Gr, Gc, M , N and Sc

In Fig.2 (b) the transient velocity profiles for different values of N, Sc and K at a particular time $t = 0.75$ are shown. The radiation parameter *N* (i.e., Stark number) defines the relative contribution of conduction heat

transfer to thermal radiation transfer. An increase in N corresponds to an increase in the relative contribution of conduction heat transfer to thermal radiation heat transfer. It can be seen that as N increases from N=2 to N=5 considerable reduction is observed in the velocity. The Schmidt number *Sc* signifies the relative effectiveness of momentum and mass transport by diffusion in the velocity and concentration (species) boundary layers. It is observed that as the Schmidt number increases the velocity decreases. The permeability co-efficient stimulates the effect of bulk matrix impedance due to porous medium fibers. A rise in the permeability coefficient enhances the velocity of the fluid.

In Fig.2(c), the transient and steady state velocity profiles are presented for different values Gr, *Gc*, *M*, *N* and *Sc*. The steady state velocity increases with an increase in *Gr* or *Gc*. It can be seen that an increase in the thermal or species buoyancy force, reduces the time to reach the steady state. The steady state velocity decreases with an increase in *M* or *N* or *Sc*. The time taken to reach the steady state velocity increases as *M* or *N* increases.

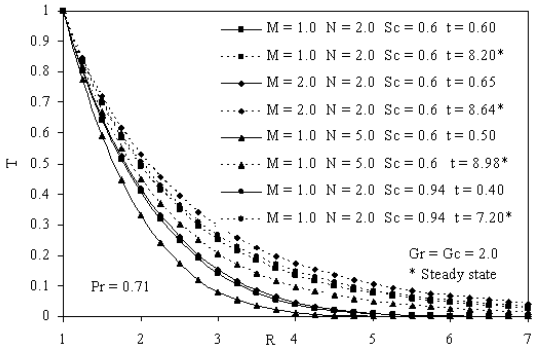


Fig.3: Temperature profiles at X=1.0 for different M, N and Sc

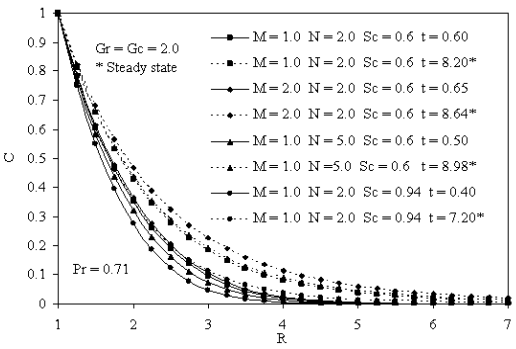


Fig. 4: Concentration profiles at X=1.0 for different M, N and Sc

The transient and steady state temperature profiles are presented for different values *M*, *N* and *Sc* in Fig.3. It is observed that, as *N* decreases from 5.0 to 2.0, the temperature increases markedly throughout the length of the cylinder. As a result the thermal boundary layer thickness is decreasing due to a rise in *N* values. It is noticed that the temperature decreases with an increase in *M* while it increases with an increase in *Sc*. The time required to reach the steady state temperature increases with an increase in *M* or *N* and it decreases with an increase in *Sc*.

In Fig.4, the transient and steady state concentration profiles are presented for different values of *M*, *N* and *Sc*. It is found that the concentration decreases as the radiation parameter *N* or the Schmidt number *Sc* increases, while it increases with an increase in *M*. The time required to reach the steady state concentration increases with an increase in *M* or *N* and it decreases with an increase in *Sc*.

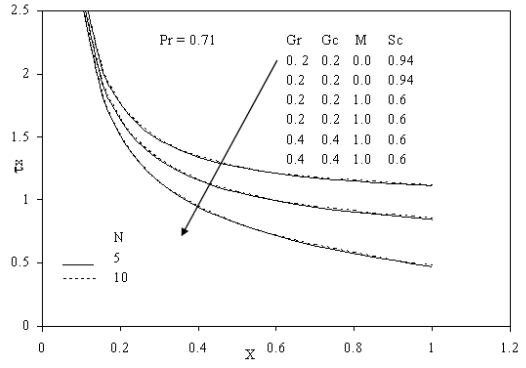


Fig. 5: Local skin friction

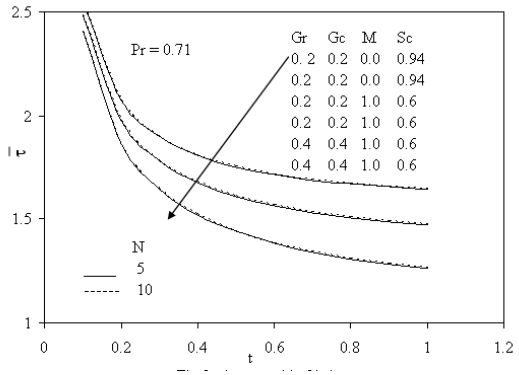


Fig. 6: Average skin friction

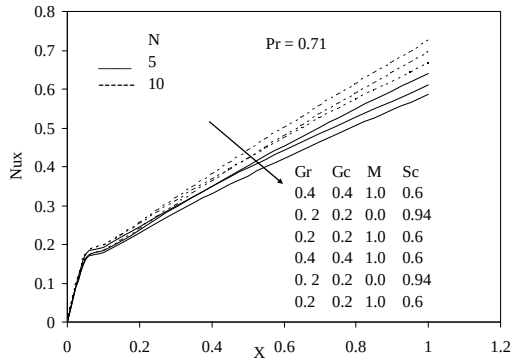


Fig. 7: Local Nusselt number

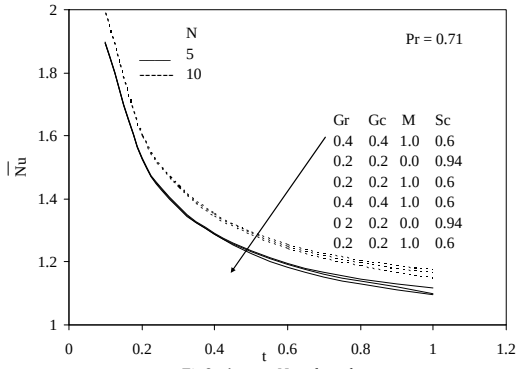


Fig. 8: Average Nusselt number

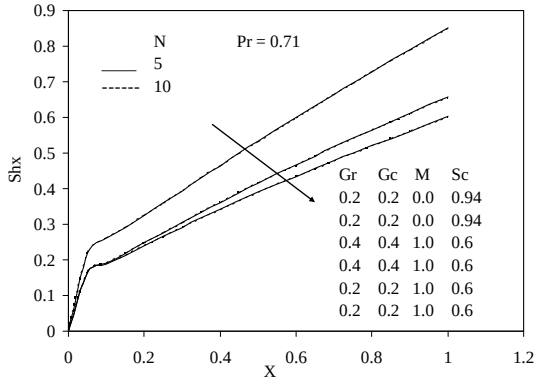


Fig. 9: Local Sherwood number

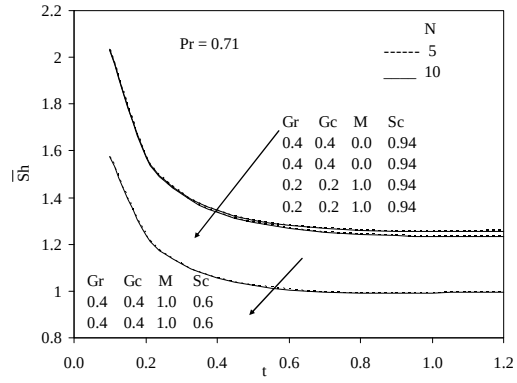


Fig. 10: Average Sherwood number

Steady-state local skin-friction ($\tau_x$) values against the axial coordinate X are plotted in Fig.5. The local shear stress $\tau_x$ increases with an increase in *Sc* ,while it decreases with an increase in *Gr* or *Gc* or *M*. The average skin-friction ($\bar{\tau}$) values are shown in Fig. 6. It is found that the average skin-friction increases with an increase in *Sc*, while it decreases with an increase in *Gr* or *Gc* or *M*, throughout the transient period. It is also observed that the average skin-friction increases as the radiation interaction parameter *N* increases. The local Nusselt number ($Nu_X$) is shown in Fig.7. The local heat transfer rate decreases with an increase in *Sc*, while it increases with an increase in *Gr* or *Gc* or *M*. Also it is found that as the radiation parameter *N* increases, the local Nusselt number increases. The average Nusselt number ($\overline{Nu}$) values are shown in Fig.8. It is observed that the average Nusselt number increases with an increase in *Gr* or *Gc* or *N*. The local Sherwood number $Sh_X$ is plotted in Fig.9. It is noticed that $Sh_X$ increases with an increase in *Sc*, where as it decreases with an increase in *Gr* or *Gc* or *N*. The average Sherwood number ($\overline{Sh}$) values are shown in Fig.10. It can be seen that the average Sherwood number increases with an increase in *Gr* or *Gc* or *Sc*, while it decreases with an increase in *M* .

## 5. Conclusion

A numerical study has been carried out to study the radiation and mass transfer effects on MHD flow of an incompressible viscous fluid past a moving vertical cylinder in a porous medium. The fluid is gray, absorbing-emitting but non-scattering medium and the Rosseland approximation is used to describe the radiative heat flux in the energy equation. A family of governing partial differential equations are solved by an implicit finite difference scheme of Crank-Nicolson type, which is stable and convergent. The results are obtained for different values of radiation parameter *N*, thermal Grashof number *Gr*, solutal Grashof number *Gc*, magnetic field parameter *M*, and Schmidt number *Sc*. Conclusions of this study are as follows:

1. The time required for velocity to reach the steady-state increases as radiation parameter *N* increases.
2. As small values of the radiation parameter *N*, the velocity and temperature of fluid increases sharply near the cylinder as the time *t* increases, which is totally absent in the absence of radiation effects.
3. The transient velocity increases with the increase in the permeability co- efficient K.
4. The skin-friction decreases with an increase M and increases with the increasing value of radiation parameter *N* and Schmidt number *Sc*.
5. The average Nusselt number increases with the increasing value of the radiation parameter.
6. The average Sherwood number increases as *Gr* or *Gc* and *Sc* increases.

## References

Brewster, M.Q. (1992): Thermal radiative transfer and properties, John Wiley & Sons, New York. Carnahan, B., Luther H.A.and Wilkes J.O. (1969): Applied Numerical Methods, John Wiley & Sons, New York. Evan L.B., Reid R.C. and Drake E.M. (1968): Transient natural convection in a vertical cylinder, A.I.Ch.E. J., Vol.14, pp.251-261.

Ganesan, P. and Rani, H.P. (2000): Unsteady free convection MHD flow past a vertical cylinder with heat and mass transfer, Int. J. Therm. Sci., Vol.39, pp.265-272. doi:10.1016/S1290-0729(00)00244-1.

Ganesan, P. and Loganathan, P.(2002): Radiation and mass transfer effects on flow of an incompressible viscous fluid past a moving vertical cylinder, Int. J. Heat Mass Transfer, Vol. 45, pp.4281-4288. doi:10.1016/S0017-9310(02)00140-0.

Ganesan, P.and Loganathan, P. (2003): Magnetic field effect on a moving vertical cylinder with constant heat flux, Heat Mass Transfer, Vol.39, pp.381-386.

Gnaneshwar, M. and Bhaskar Reddy, N. (2009): Radiation and mass transfer effects on unsteady MHD free convection flow of an incompressible viscous fluid past a moving vertical cylinder, accepted for the Journal of Theorotical and Applied Mathematics.

Hossain M.A, Kuttubuddin, M. and Pop,I. (1999): Radiation-conduction interaction on mixed convection from a horizontal circular cylinder, Heat Mass Transfer, Vol. 35, pp.307-314.

Ingham, D. and Pop, I. (Eds). (2002): Transport phenomena in porous Media II, pergamon, Oxford Kaviany, M. (1992): Principles of Heat Transfer in Porous Media, MacGraw-Hill, New York.

Kambiz Vafai, K. (Ed). (2005): Hand Book of Porous Media,Marcel Dekker, New York.

Michiyoshi, I., Takahashi, I. and Seizawa, A. (1976) :Natural convection heat transfer form a horizontal cylinder to mercury under a magnetic field, Int. J. Heat Mass Transfer, Vol.19, pp.1021-1029. doi:10.1016/0017-9310(76)90185-X

Mosa, M.F.(1979): Radiative heat transfer in horizontal magnetohydrodynamic channel flow with buoyancy effects and an axial temperature gradient, PhD Thesis, Mathematics Department, Bradford University, England, UK.

Nield, D.A and Bejan, A.(2006): Convection in Porous media, 3rd Edn. Springer, New York.

Nasser, S. Elgazery and Hassan, M.A. (2007): Numerical study of radiation effect on MHD transient mixed-convection flow over a vertical cylinder with constant heat flux.,communications in numerical methods engineering, vol.24, issue 11, pp.1183-1202.

Ramachandra Prasad V., Bhaskar Reddy, N. and Muthucumaraswamy, R. (2007): Radiation and mass transfer effects on Two-dimensional flow past an impulsively started isothermal vertical plate, Int. J. Thermal Sciences, Vol.49, pp.1251-1258. doi:10.1016/j.ijthermalsci.2007.01.004.

Shanker, B.and Kishan, N.(1997): The effects of mass transfer on the MHD flow past an impulsively started infinite vertical plate with variable temperature or constant heat flux, J. Engg. Heat Mass Transfer, Vol.19, pp.273-278.

Velusamy, K. and Garg, V.K. (1992): Transient natural convection over a heat generating vertical cylinder, Int. J. Heat Mass Transfer, Vol.35, pp.1293-1306. doi:10.1016/0017-9310(92)90185-U.

Yih, K.A. (1999): Radiation effects on natural convection over a vertical cylinder embedded in porous media, Int. Comm. Heat Mass Transfer, Vol.26(2), pp.259-267. doi:10.1016/S0735-1933(99)00012-3.